Burns & Trauma, 2024, 12, tkad064
https://doi.org/10.1093/burnst/tkad064
Research Article

OXFORD

Research Article

miR-125b-5p delivered by adipose-derived stem cell exosomes alleviates hypertrophic scarring by suppressing Smad2

Chaolei Xu[1,†], Hao Zhang[1,†], Chen Yang[2,†], Ying Wang[1,†], Kejia Wang[1], Rui Wang[3], Wei Zhang[2], Chao Li[2], Chenyang Tian[1], Chao Han[1], Mengyang Li[1], Xu Liu[1], Yunwei Wang[1], Yan Li[1], Jian Zhang[1], Yu Li[1], Liang Luo[1], Yage Shang[1], Lixia Zhang[1], Yuxi Chen[1], Kuo Shen[1,*] and Dahai Hu[1,*]

[1]Department of Burns and Cutaneous Surgery, Xijing Hospital, Fourth Military Medical University, Xi'an 710032, China, [2]Department of Plastic Surgery, Burns and Cosmetology, The First Affiliated Hospital of Xi'an Medical University, Xi'an 710032, China and [3]Department of Aerospace Medical Training, School of Aerospace Medicine, Fourth Military Medical University, Xi'an 710032, China

*Correspondence. Dahai Hu, Email: hudhai@fmmu.edu.cn; Kuo Shen, Email: 1255725433@qq.com

[†]These authors contributed equally to this work.

Received 12 July 2023; Revised 8 December 2023; Accepted 14 December 2023

Abstract

Background: Hypertrophic scarring is the most serious and unmet challenge following burn and trauma injury and often leads to pain, itching and even loss of function. However, the demand for ideal scar prevention and treatment is difficult to satisfy. We aimed to discover the effects and mechanisms of adipose-derived stem cell (ADSC) exosomes in hypertrophic scarring.

Methods: ADSC exosomes were isolated from the culture supernatant of ADSCs and identified by nanoparticle tracking analysis, transmission electron microscopy and western blotting. The effect of ADSC exosomes on wound healing and scar formation was detected by the wound model of BALB/c mice. We isolated myofibroblasts from hypertrophic scar tissue and detected the cell viability, proliferation and migration of myofibroblasts. In addition, collagen formation and fibrosis-related molecules were also detected. To further disclose the mechanism of ADSC exosomes on fibrosis in myofibroblasts, we detected the expression of Smad2 in hypertrophic scar tissue and normal skin and the regulatory mechanism of ADSC exosomes on Smad2. Injection of bleomycin was performed in male BALB/c mice to establish an *in vivo* fibrosis model while ADSC exosomes were administered to observe their protective effect. The tissue injury of mice was observed via hematoxylin and eosin and Masson staining and related testing.

Results: In this study, we found that ADSC exosomes could not only speed up wound healing and improve healing quality but also prevent scar formation. ADSC exosomes inhibited expression of fibrosis-related molecules such as α-smooth muscle actin, collagen I (COL1) and COL3 and inhibited the transdifferentiation of myofibroblasts. In addition, we verified that Smad2 is highly expressed in both hypertrophic scar tissue and hypertrophic fibroblasts, while ADSC exosomes downregulated the expression of Smad2 in hypertrophic fibroblasts. Further regulatory mechanism analysis revealed that microRNA-125b-5p (miR-125b-5p) is highly expressed in ADSC exosomes and binds to the 3′ untranslated region of Smad2, thus inhibiting its expression. *In vivo* experiments also

© The Author(s) 2024. Published by Oxford University Press.
This is an Open Access article distributed under the terms of the Creative Commons Attribution Non-Commercial License (https://creativecommons.org/licenses/by-nc/4.0/), which permits non-commercial re-use, distribution, and reproduction in any medium, provided the original work is properly cited. For commercial re-use, please contact journals.permissions@oup.com

Downloaded from academic.oup.com/burnstrauma/article/doi/10.1093/burnst/tkad064/7676325 by guest on 13 October 2026

revealed that ADSC exosomes could alleviate bleomycin-induced skin fibrosis and downregulate the expression of Smad2.
Conclusions: We found that ADSC exosomes could alleviate hypertrophic scars via the suppression of Smad2 by the specific delivery of miR-125b-5p.

Key words: Adipose-derived stem cell, Exosomes, Hypertrophic scar, miR-125b-5p, Smad2, MicroRNA, Skin, Fibrosis

Highlights

- ADSC exosomes promote wound healing, improve healing quality and alleviate hypertrophic scarring.
- ADSC exosomes can alleviate hypertrophic scarring by regulating the TGF-β/Smad signaling pathway.
- Highly expressed miR-125b-5p in ADSC exosomes directly inhibits expression of Smad2 and alleviates hypertrophic scarring.

Background

Hypertrophic scarring (HS) is a complicated disease that is most commonly found in patients who undergo surgery [1]. In addition, HS is the most serious and unmet challenge following burn and trauma injury, and as many as 70% of patients develop hypertrophic scars [2]. HS features excessive hyperplasia repair and deposition of collagen protein in dermis tissue after injury to the dermis or deep tissue [3]. In addition, pain, itching and even loss of function are the most reported complaints, which often result in serious physical and psychosocial disorders in HS patients [4]. Therefore, quality of life is significantly reduced by the functional and psychosocial sequelae of HS, leading to prolonged reintegration into society. Hence, HS places an enormous burden on the health care system. It is therefore pressing to explore approaches to minimize scar formation and optimize treatment. However, the demand for ideal scar prevention and treatment is difficult to satisfy. Hence, further elucidation of the molecular mechanisms underlying scar formation and prevention is paramount.

Injuries in the dermis and delayed healing are the most common reasons for the formation of HS [5,6]. Therefore, in terms of the prevention of HS, it is crucial to prevent infection and optimize the healing potential of wounds [7]. In the course of wound healing, fibroblasts play an important role and are responsible for wound contraction as well as collagen synthesis and secretion [8]. However, in the development of HS, fibroblasts transdifferentiate into myofibroblasts and express α-smooth muscle actin (α-SMA) after being stimulated in chronic wounds [9]. Myofibroblasts are characterized by increased cell viability and function, such as contraction, synthesis and secretion of collagen [10]. During wound healing, myofibroblasts function controllably and exist transiently and then they gradually undergo apoptosis [11]. However, the persistent existence of myofibroblasts leads to excessive collagen deposition and eventually HS. Hence, prolonged activation of myofibroblasts can result in collagen metabolism disturbances. Suppression of the transdifferentiation and overactivity of myofibroblasts is a vital method for the prevention of HS.

Adipose-derived stem cell (ADSC) exosomes, extracellular vesicles with a diameter of 30–150 nm, are an important means of intercellular communication [12]. Almost all cells can secrete exosomes, which contain abundant components such as lipids, proteins and nucleic acids [13]. Once exosomes are taken up by other cells, their components exert corresponding regulatory effects depending on the source of the exosomes. Therefore, similar to ADSC, exosomes can protect tissues from certain wounding agents and promote the regeneration of damaged tissue [14,15]. Notably, ADSC exosomes could not only promote wound healing but also improve healing quality and remit HS [16]. Emerging studies have focused on the regulatory effect of mesenchymal stem cell (MSC) exosomes on myofibroblast transdifferentiation [17,18]. In addition, our previous results indicated that ADSC exosomes could alleviate HS by downregulating the expression of the PI3K/AKT pathway and the IL-17a/Smad2 axis in myofibroblasts [16,19]. However, in-depth and comprehensive research should be conducted to elucidate the mechanism underlying the regulatory effect of ADSC exosomes on HS.

In this study, we explored the protective effect of ADSC exosomes on wound healing and HS and revealed a possible mechanism. We found that ADSC exosomes could not only speed up wound healing, but also mitigate HS. ADSC exosomes downregulated the expression of fibrosis-related molecules, as well as Smad2. Further bioinformatics analysis and inhibition experiments revealed that highly expressed microRNA-125b-5p (miR-125b-5p) in ADSC exosomes could directly bind to the 3′ untranslated region (3′UTR) of Smad2 and inhibit its expression, hence improving HS. Collectively, this study revealed that ADSC exosomes inhibit fibrosis in myofibroblasts and improve HS via delivery of miR-125b-5p.

Methods

Ethical approval

Hypertrophic scar tissue, normal full-thickness skin tissue and adipose tissue were obtained from patients (mean age 35 years) undergoing surgery in the Department of Burns

Downloaded from academic.oup.com/burnstrauma/article/doi/10.1093/burnst/tkad064/7676325 by guest on 13 October 2026

and Cutaneous Surgery, Xijing Hospital (Xi'an, China). Prior to surgery, all patients were informed of the purpose and procedure of the study and agreed to provide the tissue that should be removed for their surgery. All participants in the experiment signed a written informed consent form and the study was approved by the Ethics Committee of Xijing Hospital, Fourth Military Medical University.

Extraction and culture of hypertrophic scar fibroblasts

Extraction of hypertrophic scar fibroblasts was performed as previously reported [20]. The hypertrophic scar tissue was collected and treated on a sterile bench with a scalpel to separate and remove the epidermis and subcutaneous tissue, followed by digestion of the cells with 0.2% collagenase type I (Sigma, Germany) at 37°C for 0.5–1 h. The digested cells were passed through 100 and 70 μm cell filters, followed by the addition of Dulbecco's modified Eagle's medium (DMEM; Gibco, USA) containing 10% fetal bovine serum to stop the digestion, centrifuged at 300 × g for 5 min, resuspended in cell culture flasks, cultured and passaged at 5% CO_2 and 37°C. Third- to fifth-generation fibroblasts were used for subsequent experiments.

Extraction and identification of human adipose stem cells

Human subcutaneous adipose tissue was removed from the fascia and blood vessels, placed in glass jars, cut up as much as possible and then digested by shaking in a 0.2% solution of collagenase type I (Gibco, Grand Island, USA, Cat. 17 100–017) at 37°C. Subsequently, the mixture was filtered, centrifuged and resuspended in human ADSC-specific medium (OriCell medium, Cyagen, China). ADSC from generations 3–5 were incubated with fluorescently coupled antibodies (anti-CD29-FITC, anti-CD44PE, anti-CD73-FITC, anti-CD90-FITC, anti-CD34-PE and anti-CD45-FITC) and detected by flow cytometry (BD FACSAria™ III system; BD Pharmingen). Six-well cell culture plates were precoated with 0.1% gelatin solution, followed by lipogenic and osteogenic induction of differentiation at 90–100% confluence and 60–70% confluence (Cyagen Bioscience, Inc., Guangzhou, China). And then, ADSC were then cultured in 6-well plates with lipogenic differentiation induction medium for 2 weeks and osteogenic differentiation induction medium for 3 weeks. The ADSC were fixed in 4% paraformaldehyde after lipogenesis and osteogenesis induction, stained with Oil Red O and Alizarin Red to view the induction results, and the images were observed under an Olympus IX71 light microscope (Tokyo, Japan).

Extraction, identification and labeling of human adipose stem cell exosomes

Human ADSC were cultured in 175 cm^2 cell culture flasks in exosome-free serum medium (FBS was ultracentrifuged at 100,000 × g for 18 h to remove cellular exosomes from bovine serum). Conditioned culture medium was collected for exosome extraction by differential ultracentrifugation as previously reported [21,22]. All centrifugation steps were performed at 4°C. First, sediment was removed by centrifugation at 300 x g for 10 min. Next, the supernatant was centrifuged at 2000 x g for 10 min to remove cell debris and apoptotic vesicles. The supernatant was then centrifuged at 10,000 x g for 30 min, followed by centrifugation at 100,000 x g for 90 min using a Ti70 rotor (Optima XPN-100 Ultracentrifuge, Beckman Coulter, Kraemer Boulevard Brea, USA). The precipitated exosomes were resuspended in 100 μl of phosphate-buffered saline (PBS) and the morphology and size of the extracted exosomes were immediately observed by transmission electron microscopy (TEM) and nanoparticle tracking analysis (NTA; ZetaView® system). Simultaneous immunoblotting was performed to detect the expression of the known exosome markers CD9 and CD63. Exosomal protein concentrations were measured using a BCA protein assay kit, with an average concentration of 2 μg/μl. Exosomes were diluted in complete medium and decontaminated with a 0.22 μm filter before the experiment. Purified exosomes were labeled with the red fluorescent dye PKH26 to detect phagocytosis in hypertrophic scar fibroblasts (HSFs) (Sigma Aldrich, St. Louis, USA). Briefly, 250 μl of exosomes diluted in PBS were incubated with PKH26 at a final concentration of 1×10^{-6} M for 5 min. HSFs were stimulated with PKH26-labeled exosomes in serum-free medium for 24 h and fixed in 4% paraformaldehyde. Cells were washed three times with PBS, nuclei were stained with DAPI and images were captured with FSX100 microscope (Olympus, Tokyo, Japan).

Cell transfection of hsa-miR-125b-5p mimic and inhibitor

HSFs were grown in 6-well plates and transfected with synthetic RNA (100 mM per well of diluted hsa-miR-125b-5p mimic, hsa-miR-125b-5p inhibitor and negative control) using Lipofectamine 2000 (Invitrogen, Carlsbad, CA, USA). After 24 or 48 h of transfection, cells were harvested for analysis. Carboxyfluorescein (FAM)-modified 2-OMe-oligonucleotides were chemically synthesized and purified using high-performance liquid chromatography (GenePharma, Shanghai, China). All transfections were performed in triplicate. mRNA or protein levels were assayed. The expression of fibrosis markers [Smad2, collagen I (COL1), COL3 and α-SMA] was analyzed.

Quantitative real-time polymerase chain reaction

Samples were dissolved in TRIzol reagent (Takara, Japan), total RNA was extracted and the concentration was quantified. A total of 500 ng of RNA was reverse transcribed to cDNA using a Prime Script™ RT kit (Takara, Japan). cDNA was reverse transcribed to cDNA using Ultra SYBR mix (CWBIO, Beijing, China) and specific primers and then analyzed using a Bio-Rad IQ5 real-time analysis system (Bio-Rad, Hercules, CA, USA) with specific primers. The reaction mixture was predenatured at 95°C for 10 min, denatured at 95°C for 15 s, annealed at 60°C for 1 min and entered a melting-curve phase with 40 cycles of amplification. Relative

Downloaded from academic.oup.com/burnstrauma/article/doi/10.1093/burnst/tkad064/7676325 by guest on 13 October 2026

expression levels were calculated using the 2-ΔΔCT method. Each reaction was performed in triplicate to obtain normalized expression levels of the target gene for GAPDH. For miRNA, 600 ng of RNA was transcribed into cDNA using a reverse transcription kit (Mir-X™ miRNA First-Strand Synthesis) available from Clontech. Real time polymerase chain reaction (RT–PCR) was performed using the miScript SYBR Green PCR kit and miRNA-specific primers. U6 was used as an internal control.

Western blotting

To extract proteins from cells and tissues, fibroblasts and scar tissue were collected, washed twice with PBS and lysed in cell lysis buffer (RIPA, Beyotime) supplemented with protease inhibitors (PMSF, China Bost). After lysis the samples were incubated on ice for 15 min. Cell debris was then removed by centrifugation at 12,000 x g for 5 min at 4°C. The protein concentration was determined using a BCA kit (Beyotime). Total protein (50 μg)_was run on a 10% SDS-PAGE gel and transferred to a PVDF transfer membrane (Millipore, Billerica) at 100 V for 40–100 min. The membrane was then blocked with 5% skim milk for 1 h at room temperature in TBST and probed with the following antibodies: COL1 (1 : 1000, Abcam, Cambridge, UK), COL3 (1 : 1000, Abcam, Cambridge, UK), α-SMA (1 : 1000, CST, USA), CD9, CD63 (1 : 1000, Proteintech, China), Smad2 antibody sampling kit (1 : 1000, CST) and β-actin (1 : 1000, Xi'an Johnson & Johnson) and incubated overnight at 4°C. The next day, the samples were incubated with enzyme-labeled anti-rabbit IgG secondary antibody (1 : 3000, Bots, Wuhan, China) for 1 h at 37°C. Proteins were detected by chemiluminescence with an ECL kit (ECL Kit, MA, USA), immunoblotting of membranes was probed with a FluorChem FC system (Alpha Innotech), protein expression intensity was analyzed with ImageJ software and β-actin was used to normalize.

Wound scratch test and Transwell assay

HSFs were cultured in 6-well cell culture plates and starved with serum-free medium for 12–16 h prior to stimulation with ADSC exosomes (20 μg/ml). Monolayers of cells were scored into straight notches with a 200 μl sterile pipette tip, rinsed three times with PBS and treated with ADSC exosomes or an equivalent amount of PBS. After 0, 12 and 24 h, the distance of the scratch border was measured along the four points of the scratch using Image-Pro Plus 6.0 software.

The HSFs cell suspension was inoculated at a density of 2 x 10^4/well into the upper chamber of a 24-well transfer plate (Corning, NY) with a filter membrane pore size of 8 μm by adding 500 μl of medium containing de-FBS. Medium (1 ml) supplemented with ADSC exosomes (20 μg/ml) or an equivalent volume of PBS was added to the lower chamber and incubated for 24 h. HSFs were then fixed with 4% paraformaldehyde for 30 min and washed three times with PBS. HSFs were stained with 0.5% crystalline violet staining solution (500 μl, Boster) and incubated for 10 min at room temperature. After washing with PBS, the number of migrating cells was observed under a microscope (FSX100, Olympus, Tokyo, Japan).

Immunofluorescence staining

HSFs with different treatments were cultured in 6-well cell culture plates for 24 h. HSFs were fixed in 4% paraformaldehyde for 15 min at room temperature, washed three times with PBS, permeated with 0.1% Triton X-100 in PBS for 20 min and blocked with 2% BSA in PBS for 1 h. Primary antibodies (α-SMA, 1 : 200, CST; ki67, 1 : 200, CST; and Smad2 1 : 200, CST) were diluted in 2% BSA and incubated overnight at 4°C. The next day, the HSFs were incubated with an anti-rabbit secondary antibody (1 : 200) for 1 h at 37°C and counterstained with DAPI and images were obtained on an Olympus FSX100 microscope.

Luciferase reporter assay

To confirm that Smad2 is indeed a direct target of miR-125b-5p, a luciferase-3′-UTR reporter construct for Smad2 mRNA was obtained from HANBIO (Shanghai, China). Wild-type Smad2 3′UTR, mutant Smad2 3′UTR or its nontargeting control RNA was cotransfected with miR-125b-5p mimics at a final concentration of 50 nM using Lipofectamine 2000 transfection reagent. Samples were harvested after 24 h for luciferase assay (Promega, WI, USA).

Bleomycin-induced fibrosis mouse model

All animal experiments were performed in strict accordance with the animal care policy approval and system. A total of 24 male BALB/c mice (6–8 weeks old) were purchased from the Experimental Animal Centre of the Fourth Military Medical University (Xi'an, China) and fed under standard conditions. Mice were randomly divided into three groups (8 mice per group): PBS control group, 100 μl bleomycin (1 mg/ml) group and 100 μl bleomycin (1 mg/ml) + ADSC-Exo group (100 μg diluted in 100 μl of PBS). All mice in the bleomycin group and bleomycin + ADSC-Exo group were subcutaneously injected with bleomycin every day before sacrifice to establish the HS mouse model. The mice were sacrificed 4 weeks later and the lesioned skin tissues were analyzed by hematoxylin and eosin (H&E) and Masson staining.

Effect of ADSC exosomes on the wound model

Male BABL/c mice at 6–8 weeks were purchased from the Experimental Animal Centre of the Fourth Military Medical University. The animal protocols were carried out in strict accordance with the policies of the Laboratory Animal Committee of the Fourth Military Medical University (Xi'an, China). Mice were randomly divided into two groups: the PBS group and the ADSC-Exo group (100 μg diluted in 100 μl of PBS). Mice were anesthetized with isoflurane and a full-thickness skin defect of 1 x 1 cm^2 was formed on the dorsal skin. Three days later, ADSC exosomes or an equivalent volume of PBS was injected subcutaneously into the wound perimeter using a syringe for three consecutive days. Photographs of the wounds were taken on days 3, 7,

Downloaded from academic.oup.com/burnstrauma/article/doi/10.1093/burnst/tkad064/7676325 by guest on 13 October 2026

10 and 14, the mice were subsequently sacrificed and wound tissue was collected for the subsequent histological analysis. There were at least 6 mice in each experimental group (n = 6).

Histopathology analysis

Tissue samples were fixed in 4% paraformaldehyde, dehydrated in graded ethanol, embedded in paraffin and cut into 5 μm thick sections. H&E and Masson trichrome staining were used to detect histological changes and collagen deposition. For immunohistochemical staining, sections were deparaffinized and immersed in 3% H_2O_2 for 15 min at 37°C to remove terminal peroxidase activity, and blocked with 5% BSA in PBS for 1 h to eliminate nonspecific binding. The slides were then incubated overnight at 4°C with primary antibodies against α-SMA and Smad2. The next day, slides were incubated with the PV6000 Histostain™ kit (ZSGB, Beijing, China) and stained with diaminobenzidine (ZSGB, Beijing, China). Images were taken with an FSX100 Bioimaging Navigator (Olympus, Tokyo, Japan).

Statistical analysis

All data were analyzed using GraphPad 8.0 software. All experiments were repeated at least three times and data are presented as the mean ± standard deviation. Student's t test was used for comparisons between two groups, and one-way analysis of variance was used for comparisons between multiple groups, followed by Dunnett's t test for comparisons within groups. For analysis of treatment with influence of time, such as wound healing, analyzed with two-way analysis of variance. $P < 0.05$ was considered statistically significant.

Results

Characterization of ADSCs and exosomes

Primary ADSCs were isolated from adipose tissue, as shown in Figure 1a, exhibiting fibroblast-like morphology under an inverted microscope. To verify the multiple differentiation potential of isolated primary ADSC, adipogenic and osteogenic induction were conducted with P3 ADSC. Lipid droplets were observed by Oil Red O staining, and calcium deposition was observed by Alizarin Red S staining. In addition, specific MSC surface markers were analyzed by flow cytometry, including positive expression of the MSC surface markers CD29 (99.47%), CD44 (99.96%), CD73 (80.70%) and CD90 (98.17%), and negative expression of the hematopoietic stem cell surface markers CD34 (1.79%) and CD45 (2.33%) (Figure 1b). These results confirmed the characterization of ADSC. Extracellular vesicles were extracted after collecting the conditioned medium for ADSC, which was authenticated with TEM, western blotting and NTA. As shown in the TEM image (Fig 1c), particles showed a typical exosome cup-shaped morphology with a double-layer membrane structure. NTA analysis results showed that the average diameter of vesicles was 101.5 nm (Figure 1d), and western blots showed high expression of CD63, CD9 and TSG101 molecular markers in the isolated vesicles (Figure 1e). The above identification showed that the isolated vesicles were consistent with exosome parameters. As shown in Figure 1f, PKH26-labeled exosomes can be engulfed by scar fibroblasts. These results indicate successful isolation of exosomes from ADSC.

ADSC exosomes accelerated wound healing and decreased collagen deposition in a wound model of BALB/c mice

It is worth noting that the speed and quality of wound healing are closely connected with hypertrophic scars. To observe the effect of ADSC exosomes on wound healing and fibrosis of skin, we created full-thickness wounds on the backs of BALB/c mice, which are the most widely used models in wound healing and scar research. As is shown in Figure 2a, injection of ADSC exosomes around the wound significantly increased the healing of full-thickness wounds. On days 7, 10 and 14 post-wounding, the wound areas in the ADSC exosomes group were smaller than those in the control group. There were significant differences between wound areas of different groups on days 7, 10 and 14 ($p < 0.05$) (Figure 2b and c). H&E and Masson's trichrome staining were carried out to evaluate the quality of wound healing. As Figure 2d indicates, the wound areas in the ASDC exosome group were smaller than those in the control group, while the number of cutaneous appendages in the ASDC exosome group was greater than that in the control group (supplementary Figure S1, see online supplementary material). Masson and Sirius red staining results indicated that the ADSC exosomes group displayed more collagen synthesis in the basket weave orientation, while the control group displayed less collagen with a parallel arrangement (Figure 2e and f). Besides, analysis of Sirius red staining results indicated that COL3 expression in the ADSC exosome group is higher than that in the control group, while COL1 expression is lower in the ADSC exosomes group (supplementary Figure S2, see online supplementary material). More capillary formation in the ADSC exosomes group was observed in the CD31 immunohistochemical staining results (Figure 2e). Moreover, Ki67 immunofluorescence staining results indicated that ADSC exosomes could significantly increase cell proliferation capacity around wounds (Figure 2g). Therefore, the above results confirmed that ADSC exosomes could accelerate wound healing and improve healing quality, implying less fibrosis.

ADSC exosomes inhibited the proliferation and migration of HSFs and alleviated the expression of profibrotic markers in HSFs

Now that we found that ADSC exosomes could alleviate fibrosis in wound healing, we further detected their effect on hypertrophic scars. For *in vitro* experiments, we isolated HSFs from hypertrophic scar tissue and treated HSFs with or without ADSC exosomes. First, we observed the effect of ADSC exosomes on the migration and proliferation capacity of HSFs. As shown in Figure 3a and b, scratch assay results

Downloaded from academic.oup.com/burnstrauma/article/doi/10.1093/burnst/tkad064/7676325 by guest on 13 October 2026

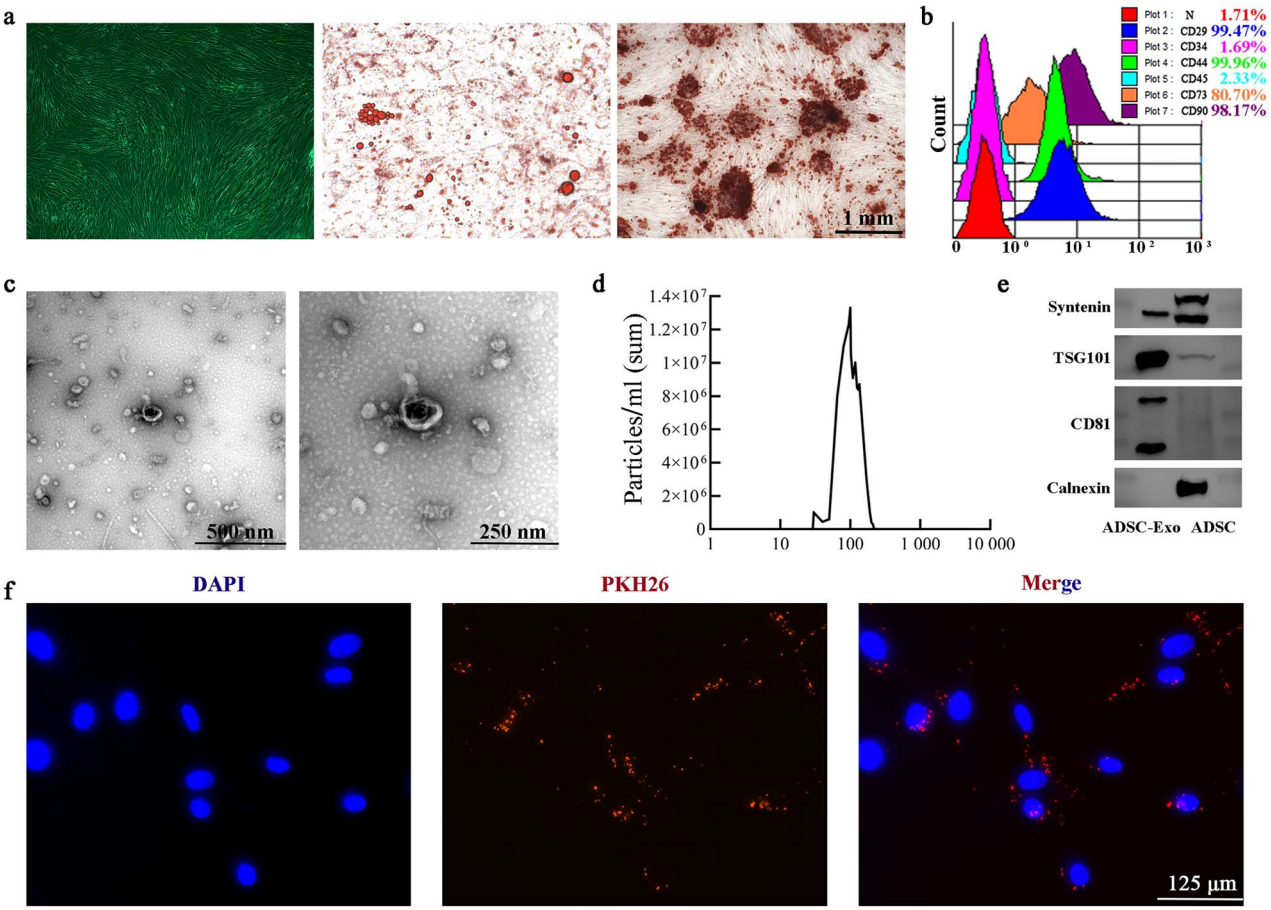

Figure 1. Characterization of adipose-derived stem cells (ADSC) and ADSC exosomes (Exo). (**a**) Morphology of ADSC observed by inverted microscopy. Oil Red O and Alizarin Red S staining showing lipid droplets and calcium deposition after adipogenic and osteogenic induction, respectively. Scale bar: 1 mm. (**b**) Flow cytometry showed that ADSC were positive for CD29 (99.47%), CD44 (99.96%), CD73 (80.70%) and CD90 (98.17%), and negative for CD34 (1.69%) and CD45 (2.33%). (**c**) Morphology of ADSC Exo detected by transmission electron microscopy. Scale bar: 500 nm (left); 250 nm (right). (**d**) Diameter distribution of ADSCs Exo detected by nanoparticle tracking analysis (nm). (**e**) Syntenin, TSG-101, CD81 and calnexin expression in ADSC Exo was detected by western blotting. (**f**) Immunofluorescence staining results of PKH26-labeled ADSC Exo on fibroblasts; blue: DAPI, red: PKH26-labeled ADSC Exo. Scale bar: 125 μm

indicated that ADSC exosomes inhibit the migration capacity of HSFs at 12, 24 and 48 h after stimulation. The proliferation capacity of HSFs was suppressed after ADSC exosomes treatment, as shown by the CCK8 assay results (Figure 3c). In addition, the Transwell assay also confirmed the influence of ADSC exosomes treatment on the migration capacity of HSFs (Figure 3d), while Ki67 immunofluorescence staining confirmed the weakened proliferation capacity of HSFs in the ADSC exosomes group (Figure 3e). These results revealed that ADSC exosomes could inhibit the proliferation and migration of HSFs. Afterward, we tested the fibrosis-related indicators COL1, COL3 and α-SMA in HSFs treated with ADSC exosomes. As shown in Figure 3f, the protein expression levels of COL1, COL3 and α-SMA were all significantly downregulated by ADSC exosomes. In addition, we labeled ADSC exosomes with PKH26 and added them to HSFs. At 24 h after ADSC exosomes treatment, we conducted α-SMA immunofluorescence staining. As shown in Figure 3g, the ratio of α-SMA-positive cells and the mean fluorescence intensity (MFI) of α-SMA were significantly decreased in HSFs treated with ADSC exosomes. These results suggested that ADSC exosomes could inhibit the proliferation and migration of HSFs and reverse the transdifferentiation of fibroblasts to myofibroblasts to alleviate hypertrophic scar fibrosis.

Smad2 plays an important role in HS

To determine the mechanism by which ADSC regulate wound healing and scar fibrosis, we analyzed the RNA transcriptome sequencing results of hypertrophic scars and normal skin reported by Liu *et al.* (GSE181540) [23]. As shown in supplementary Figure S3a (see online supplementary material), the heatmap revealed the expression of different genes in hypertrophic scars and normal skin. As many as 1529 genes were upregulated in hypertrophic scars, while 3172 were downregulated (supplementary Figure S3b). Further bioinformatics analysis was conducted to analyze the differentially expressed genes. GO enrichments indicated that DEGs are enriched in several, biological processes: the oxidation–reduction process and

Downloaded from academic.oup.com/burnstrauma/article/doi/10.1093/burnst/tkad064/7676325 by guest on 13 October 2026

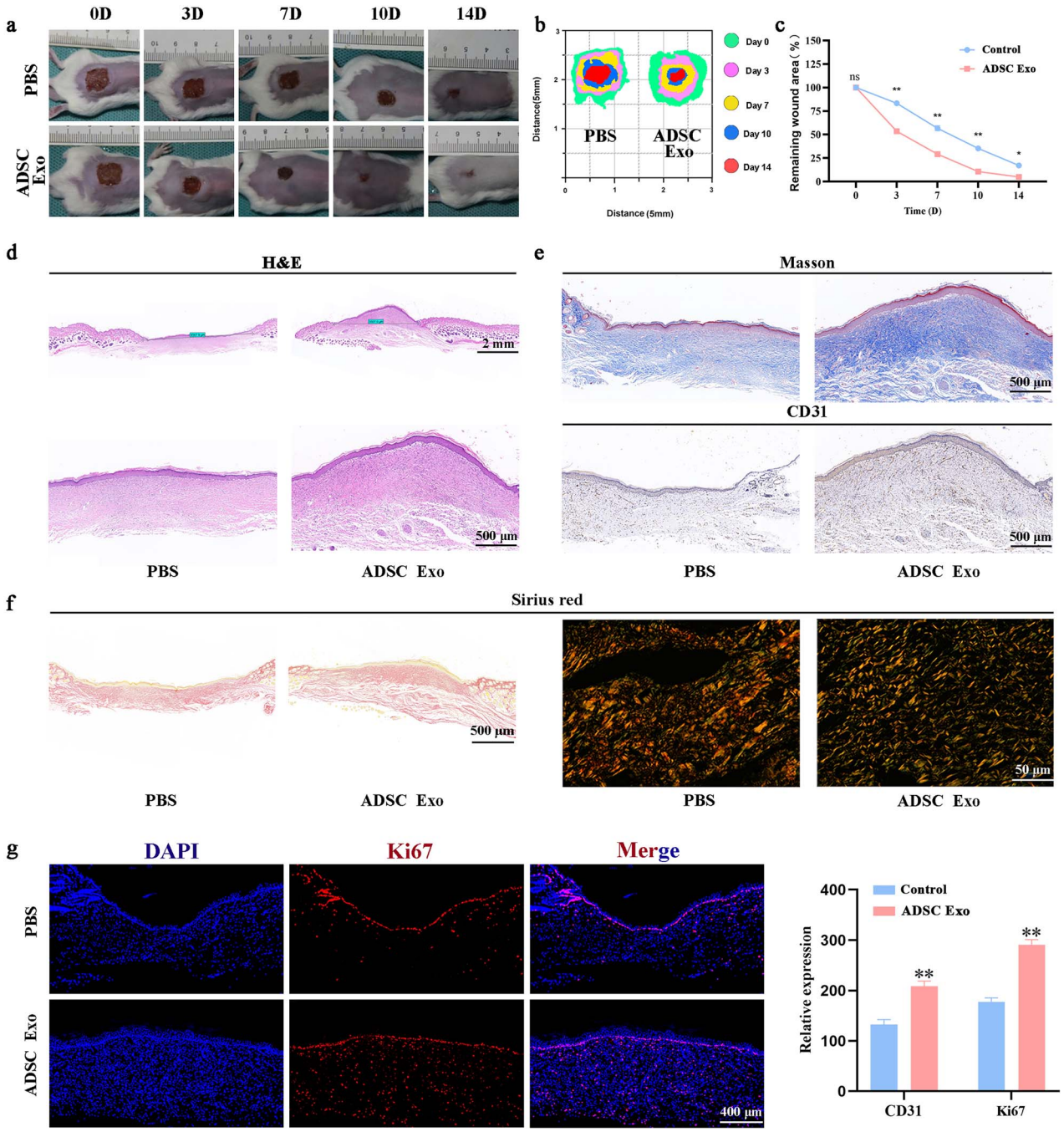

Figure 2. ADSC Exo accelerated wound healing and decreased collagen deposition in a wound model of BALB/c mice. (**a-c**) Wound area after treatment with ADSC Exo or PBS on days 0, 3, 7, 10 and 14, ns: no statistical significance, $^{*}p < 0.05$, $^{**}p < 0.01$. (**d**) H&E staining results of wounds treated with ADSC Exo or PBS. Scale bars: 2 mm or 500 μm. (**e**) Masson and CD31 immunohistochemical staining results of wounds treated with ADSC Exo or PBS. Scale bar: 500 μm. (**f**) Sirius red staining results of wounds treated with ADSC Exo or PBS. Scale bars: 500 μm or 50 μm. (**g**) Ki67 immunofluorescence staining results of wounds treated with ADSC Exo or PBS, blue: DAPI, green: Ki67, $^{**}p < 0.01$. Scale bar: 400 μm. *ADSC* adipose-derived stem cells, *Exo* exosomes, *PBS* phosphate-buffered saline, *H&E* hematoxylin and eosin

metabolic process, regulation of transcription, DNA-templated protein phosphorylation; cellular component: nucleus, membrane, nucleosome; and molecular function: DNA binding, protein binding, ATP binding, protein heterodimerization activity, TGF/Smad signal transduction system (supplementary Figure S3c). KEGG enrichment results indicated that DEGs are assembled in phenylpropanoid biosynthesis, valine, leucine and isoleucine biosynthesis, and the phosphatidylinositol signaling system (supplementary Figure S3d). Interestingly, transcriptome sequencing results confirmed that the expression of smad2, a key component in the TGF-Smad pathway that plays a

Downloaded from academic.oup.com/burnstrauma/article/doi/10.1093/burnst/tkad064/7676325 by guest on 13 October 2026

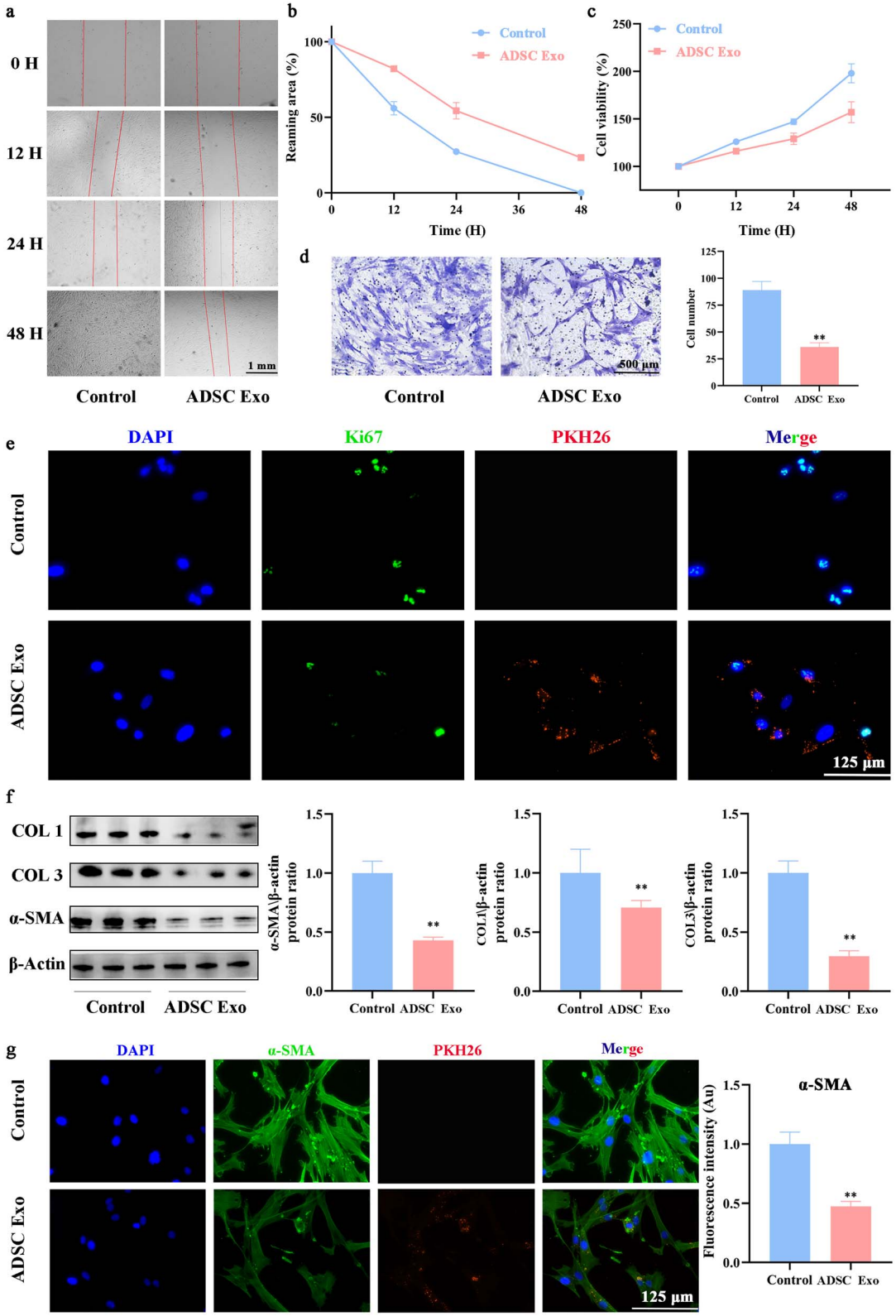

Figure 3. ADSC Exo inhibited the proliferation and migration of hypertrophic scar fibroblasts (HSFs). (**a**,**b**) The effect of ADSC Exo on HSFs migration was evaluated by scratch wound assays. Scale bar: 1 mm. (**c**) Effect of ADSC Exo on HSFs proliferation detected by CCK8. (**d**) Effect of ADSC Exo on HSFs migration evaluated by Transwell assay, $^{**}p < 0.01$. Scale bar: 500 μm. (**e**) Ki67 immunofluorescence staining results of HSFs treated with ADSC Exo or PBS; blue: DAPI, red: PKH26, green: Ki67. Scale bar: 125 μm. (**f**) α-SMA, collagen I (COL1), and collagen III (COL3) expression in HSFs treated with ADSC Exo or PBS, $^{**}p < 0.01$. (**g**) α-SMA immunofluorescence staining results of wounds treated with ADSC Exo or PBS, blue: DAPI, red: PKH26, green: α-SMA, $^{**}p < 0.01$. Scale bar: 125 μm. *ADSC* adipose-derived stem cells, *Exo* exosomes, *PBS* phosphate-buffered saline, *α-SMA* α-smooth muscle actin

Downloaded from academic.oup.com/burnstrauma/article/doi/10.1093/burnst/tkad064/7676325 by guest on 13 October 2026

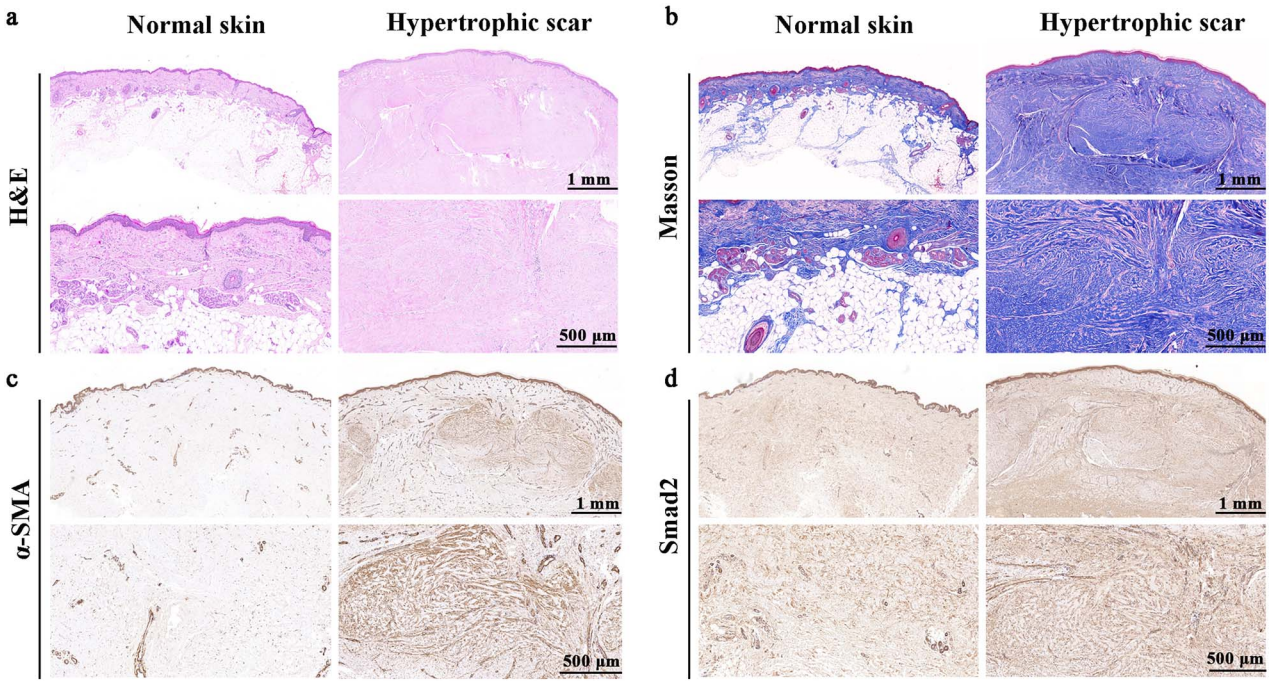

Figure 4. Smad2 plays an important role in hypertrophic scarring. (**a**) H&E staining results of tissue from normal skin and hypertrophic scars. Scale bars: 1 mm or 500 μm. (**b**) Masson staining results of tissue from normal skin and hypertrophic scars. Scale bars: 1 mm or 500 μm. (**c**) α-SMA immunohistochemical staining results of tissue from normal skin and hypertrophic scars. Scale bar: 1 mm or 500 μm. (**d**) Smad2 immunohistochemical staining results of tissue from normal skin and hypertrophic scars. Scale bars: 1 mm or 500 μm. *H&E* hematoxylin and eosin, α-*SMA* α-smooth muscle actin

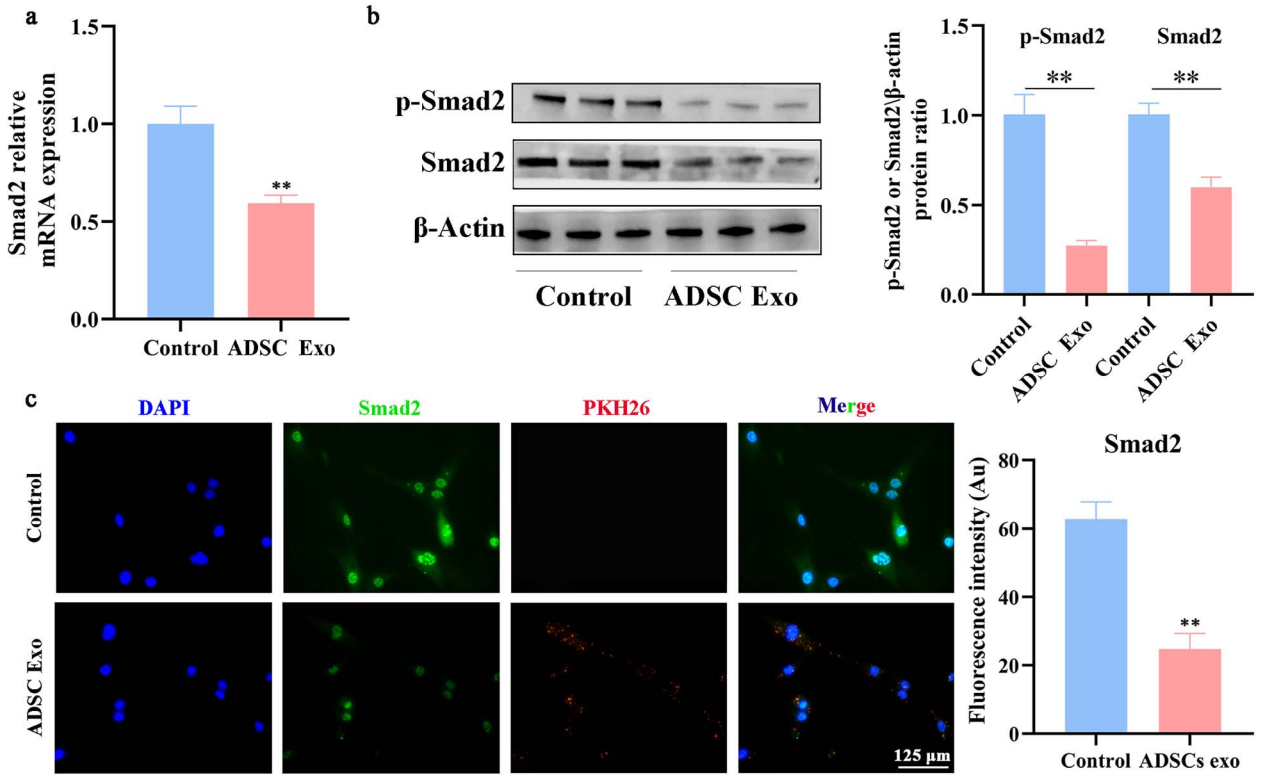

Figure 5. ADSC exosomes downregulate the expression of Smad2. (**a**) PCR results of Smad2 expression in HSFs treated with ADSC Exo and PBS, $^{**}p < 0.01$. (**b**) Western blot results of Smad2 and p-Smad2 expression in HSFs treated with ADSC Exo and PBS, $^{**}p < 0.01$. (**c**) Smad2 immunofluorescence staining results of HSFs treated with ADSC Exo and PBS, blue: DAPI, red: PKH26, green: Smad2, $^{**}p < 0.01$. Scale bar: 125 μm. *ADSC* adipose-derived stem cells, *Exo* exosomes, *PBS* phosphate-buffered saline, *HSFs* hypertrophic scar fibroblasts

Downloaded from academic.oup.com/burnstrauma/article/doi/10.1093/burnst/tkad064/7676325 by guest on 13 October 2026

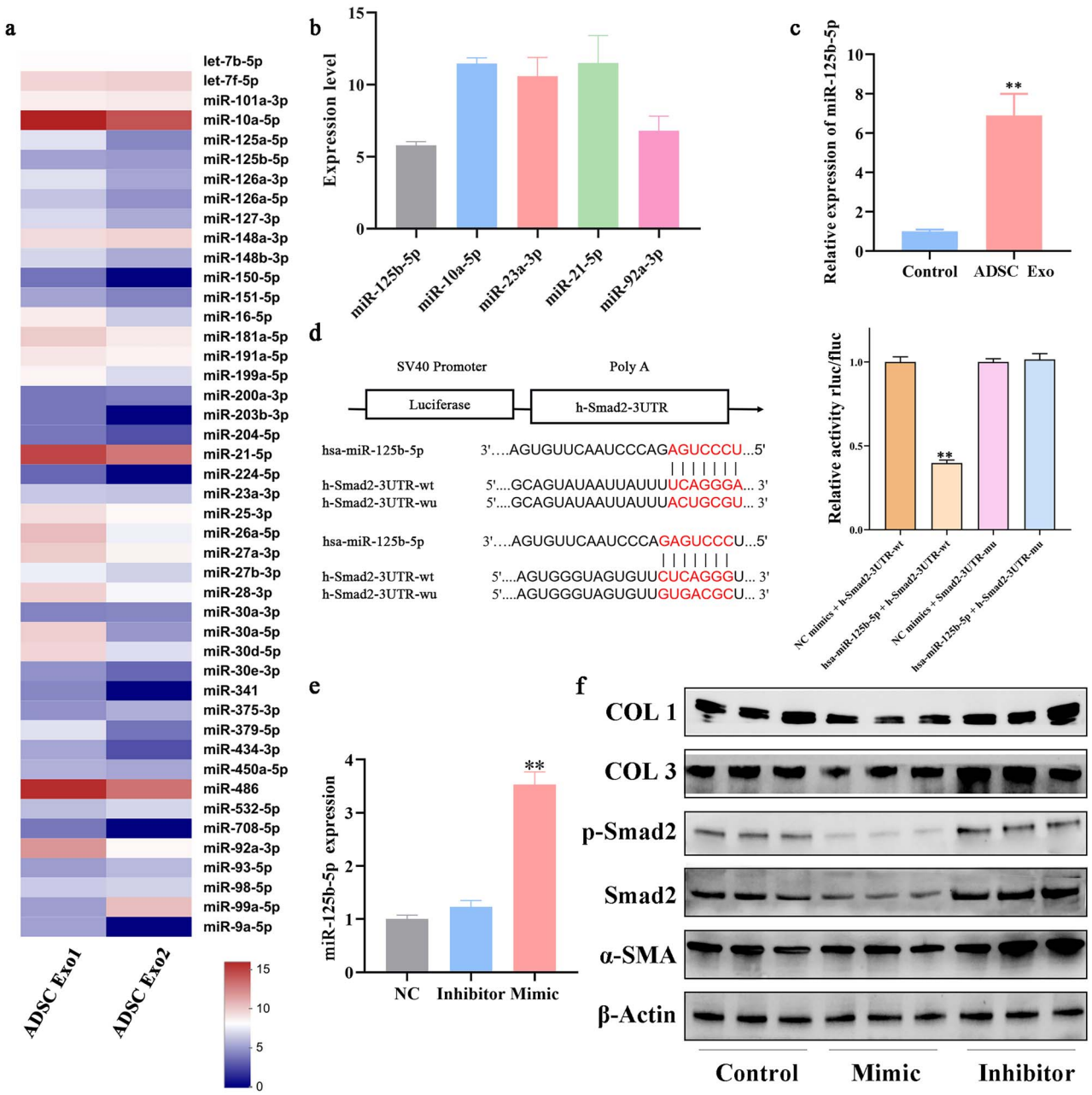

Figure 6. ADSC Exo downregulate the expression of Smad2 by delivering miR-125b-5p. (**a**) Hotmap showing miRNA microarray results of ADSC Exo. (**b**) PCR results of the expression of 5 miRNAs (miR-125b-5p, miR-10a-5p, miR-23a-3p, miR-21-5p and miR-92a-3p) in ADSC Exo. (**c**) PCR results indicating miR-125b-5p expression in PBS- and ADSC Exo-treated HSFs, $^{**}p < 0.01$. (**d**) Structure and luciferase results of the dual luciferase reporter gene, $^{**}p < 0.01$. (**e**) PCR results indicating miR-125b-5p expression in negative control (NC), miR-125b-5p expression mimic- and inhibitor-treated HSFs, $^{**}p < 0.01$. (**f**) Western blot results of α-SMA, COL1, COL3, p-Smad2 and Smad2 expression in NC, miR-125b-5p expression mimic- and inhibitor-treated HSFs.*ADSC* adipose-derived stem cells, *Exo* exosomes, *PBS* phosphate-buffered saline, H&E hematoxylin and eosin, *HSFs* hypertrophic scar fibroblasts

crucial role in the transdifferentiation of myofibroblasts, was significantly upregulated in hypertrophic scars (supplementary Figure S3e). The TGF-β/Smad2 pathway, which is overexpressed in scar tissue and causes fibrosis, plays an important role in scar fibrosis. Then, we collected skin tissues from 10 healthy patients (normal skin) and 8 hyperplastic patients (scar skin) and conducted H&E, Masson, and αSMA and Smad2 immunohistochemical staining. H&E staining indicated that the thickness of the dermis in the scar was greater than that in normal skin (Figure 4a). Masson staining results also showed increased collagen deposition and disordered arrangement in scar tissue (Figure 4b). In addition, αSMA immunohistochemical staining results indicated that the expression of αSMA was significantly upregulated in the

Downloaded from academic.oup.com/burnstrauma/article/doi/10.1093/burnst/tkad064/7676325 by guest on 13 October 2026

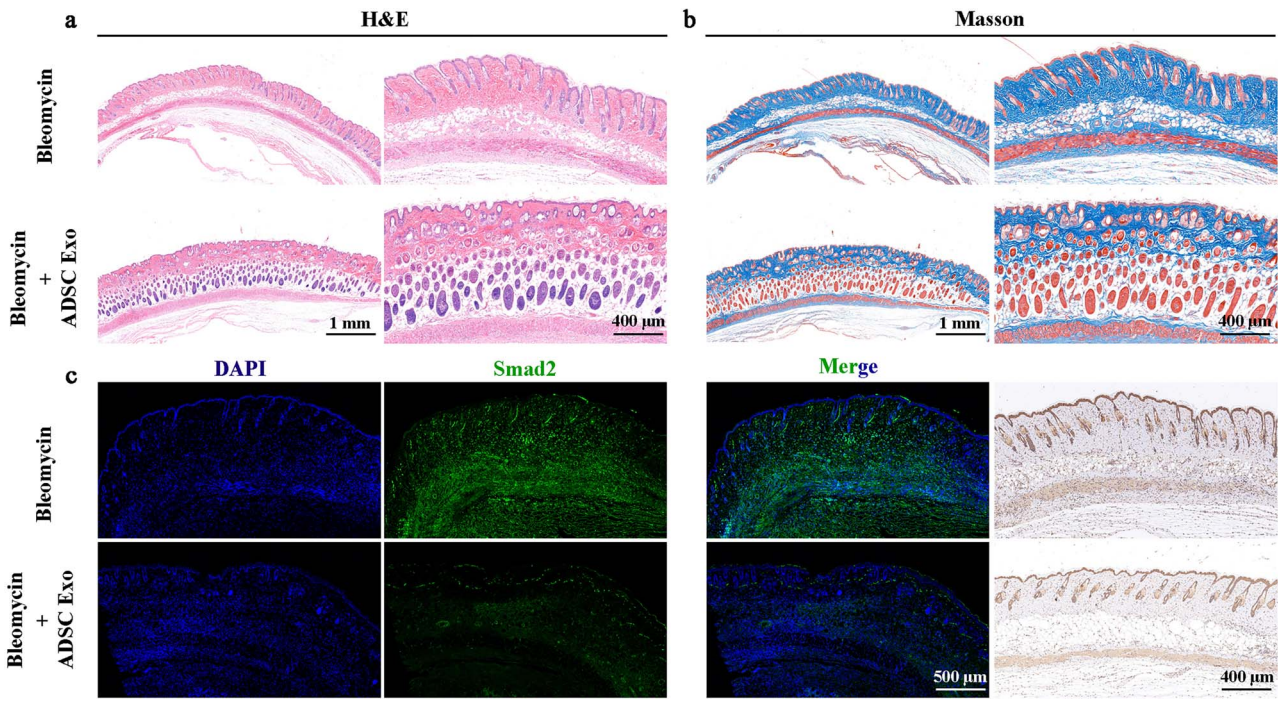

Figure 7. ADSC Exos alleviate fibrosis and decrease the expression of Smad2 in a mouse fibrosis model. (**a**) H&E staining results of ADSC Exo or PBS-treated bleomycin-induced fibrosis. Scale bars: 1 mm or 400 μm. (**b**) Masson staining results of ADSC Exo or PBS-treated bleomycin-induced fibrosis. Scale bars: 1 mm or 400 μm. (**c**) Smad2 immunofluorescence and immunohistochemical staining results of ADSC Exo or PBS-treated bleomycin-induced fibrosis, blue: DAPI, green: Smad2. Scale bars: 500 or 400 μm. *ADSC* adipose-derived stem cells, *Exo* exosomes, *PBS* phosphate-buffered saline, *H&E* hematoxylin and eosin

dermis of scar tissue, in which fibroblasts were predominant (Figure 4c). Meanwhile, as Figure 4d indicates, there is more Smad2 expression in scar tissue than in normal skin.

ADSC exosomes downregulate the expression of Smad2

To verify whether ADSC exosomes could regulate the expression of Smad2, we detected the expression of Smad2 in myofibroblasts treated with or without ADSC exosomes. As shown in Figure 5a, PCR results indicated that ADSC exosomes treatment decreased the expression of Smad2 at the mRNA level. Western blot results also showed decreased expression of both Smad2 and p-Smad2 in ADSC exosomes-treated myofibroblasts (Figure 5b). Moreover, Smad2 immunofluorescence staining results showed that when treated with ADSC exosomes, the ratio of Smad2-positive cells and the MFI of Smad2 were significantly decreased in myofibroblasts (Figure 5c). The above results indicated that ADSC exosomes could downregulate the expression of Smad2 in myofibroblasts.

ADSC exosomes downregulate the expression of Smad2 by delivering miR-125b-5p

miRNAs are crucial posttranscriptional regulators that can directly bind to the 3′UTR of mRNA and inhibit its translation. To verify the regulatory mechanism of ADSC exosomes on Smad2, we analyzed the miRNA chip results (GSE92313). As shown in Figure 6a, as many as 45 miRNAs were detected in ADSC exosomes, among which miR-125b-5p, miR-10a-5p, miR-23a-3p, miR-21-5p and miR-92a-3p were the most abundant. Next, we conducted PCR and confirmed that miR-125b-5p, miR-10a-5p, miR-23a-3p, miR-21-5p and miR-92a-3p were relatively highly expressed in ADSC exosomes (Figure 6b). Interestingly, miRbase analysis revealed that Smad2 is a potential target gene of miR-125b-5p. Then, we detected the expression of miR-125b-5p in ADSC exosomes-treated myofibroblasts. The results indicated that the expression of miR-125b-5p in ADSC exosomes-treated myofibroblasts was significantly higher than that in myofibroblasts (Figure 6c). To further verify the regulatory effect of miR-125b-5p on Smad2, we conducted a dual luciferase reporter assay. As shown in Figure 6d, overexpression of miR-125b-5p impaired the activity of the Smad2–3′UTR-wt reporter, but there was no notable activity shift within the mutated reporter. Namely, Smad2 is a regulatory target of miR-125b-5p, and miR-125b-5p can bind to the 3′UTR of the Smad2 gene. To further verify the regulatory effect of miR-125b-5p on Smad2, we designed and synthesized a mimic and inhibitor of miR-125b-5p and transfected them into myofibroblasts. As shown in Figure 6e, the expression of miR-125b-5p was significantly promoted by the mimic but remained unchanged by the inhibitor. In addition, when the expression of miR-125b-5p was increased by the mimic, the expression of Smad2 and p-Smad2 was suppressed, while the inhibitor increased the expression of Smad2 and p-Smad2 (Figure 6f and supplementary Figure 4, see online supplementary material). Collectively, the regulatory effect

Downloaded from academic.oup.com/burnstrauma/article/doi/10.1093/burnst/tkad064/7676325 by guest on 13 October 2026

of ADSC exosomes on Smad2 depends on the delivery of miR-125b-5p.

ADSC exosomes alleviate fibrosis and decrease the expression of Smad2 in a mouse fibrosis model

The above results indicated that ADSC exosomes could inhibit fibrosis and the expression of Smad2 via delivery of miR-125b-5p. To verify the antifibrotic effect of ADSC exosomes *in vivo*, we constructed a mouse fibrosis model by injecting bleomycin into the dermis of BALB/c mice for 2 weeks. After dermal fibrosis was established, 100 μg of ADSC exosomes were injected into the dermal fibrosis of mice. Seven days after ADSC exosomes treatment, skin tissues were collected for subsequent testing. H&E and Masson's trichrome staining were performed to evaluate the deposition and arrangement of collagen. H&E staining results showed a thinner epidermis and dermis as well as more hair follicles in the ADSC exosomes treatment group (Figure 7a). As shown in Figure 7b, in dermal tissue, the collagen volume fraction was significantly decreased, and the collagen arrangement was more organized in the ADSC exosomes + bleomycin group than in the bleomycin group alone; i.e. dermal fibrosis was significantly improved by ADSC exosomes. Meanwhile, Smad2 immunofluorescence and immunohistochemistry results indicated that the ratio of Smad2-positive cells and the MFI of Smad2 in the ADSC exosomes + bleomycin group were significantly decreased compared with those in the bleomycin group (Figure 7c). Thus, our results revealed that ADSC exosomes could improve the arrangement of collagen structure and proportion and decrease α-SMA-positive myofibroblasts as well as the expression of Smad2 in a bleomycin-induced fibrosis mouse model.

Discussion

HS is a common disease with a high rate of morbidity [24]. As many as 30% of patients with skin injury develop HS, while 70% of burned patients develop HS [2]. HS features excessive accumulation of extracellular matrix (ECM) and prolonged fibroblast activation and overactivity [25]. Interestingly, HS tend to form at skin injuries that reach the dermis and under the dermis [26]. It is worth noting that prolonged wound healing often results in HS, and protecting wounds from infection and accelerating concrescence is a crucial strategy to prevent HS [27]. In this study, we confirmed that ADSC exosomes could promote wound healing and increase the quality of wound healing. In addition, scar formation after ADSC exosomes treatment was greatly improved, with less collagen deposition and a more ordered arrangement. ADSC exosomes, as an important means of intercellular communication, have been reported to promote wound healing by regulating the activity of fibroblasts, vascular endothelial cells, macrophages and keratinocytes.

During wound healing, fibroblasts mainly account for collagen secretion and ECM synthesis [28]. Fibroblasts can be activated by injury or inflammation and polarized to myofibroblasts, with robust collagen synthesis activity and contractility [29,30]. There is no doubt that more collagen synthesis is beneficial to wound healing, but uncontrolled collagen synthesis leads to HS [31]. Suppression of myofibroblasts, which should have been eliminated after wound healing, is an important strategy to treat HS [32]. In this study, we isolated myofibroblasts from scar tissue and verified that ADSC exosomes could inhibit cell viability, proliferation and migration capacity as well as collagen synthesis capacity.

It is widely accepted that the polarization of fibroblasts to myofibroblasts is the key process in fibrosis, with several signaling pathways and key molecules taking part [33]. α-SMA is a marker expressed in myofibroblasts that represents robust ECM synthesis [34]. Emerging signaling pathways have been reported to participate in myofibroblast transdifferentiation and fibrosis, including TGF-β/Smad, Wnt/β-catenin and YAP/TAZ [35–37]. The TGF-β/Smad signaling pathway is a very well-described canonical signaling pathway that has been proven to play an important role in different fibrotic diseases, including renal fibrosis and HS [38]. When bound to TGF-β receptor 1, TGF-β1 triggers the phosphorylation and activation of Smad2 and Smad3. After phosphorylation, activated Smad2/3 can bind with Smad4, which enables Smad2/3 to translocate to the nucleus and transcribe specific genes, while Smad7 prevents the translocation of activated Smad2/3 [39,40]. An increasing number of studies have reported that ADSC exosomes can inhibit myofibroblast transdifferentiation by regulating several signaling pathways, such as the PI3K/AKT and TGF-β/Smad pathways [16]. Our previous results indicated that ADSC exosomes attenuated the transdifferentiation of fibroblasts to myofibroblasts by targeting IL-17RA to inhibit the phosphorylation of Smad2 in hypertrophic scar fibrosis [16]. However, in this study, we revealed that ADSC exosomes could directly downregulate the expression of Smad2. It is important to note that only phosphorylated Smad2 is activated, which can trigger downstream regulation. All previous research has focused on the inhibition of Smad2 phosphorylation and activation. In this study, we found that ADSC exosomes could directly decrease the expression of Smad2 and weaken its influence on downstream regulation.

miRNA, a kind of key noncoding RNA with a length of 18–22 nt, is one of the most important components in exosomes [41,42]. miRNAs in exosomes can transfer into receiving cells and bind to the gene's 3′UTR to regulate their expression, hence regulating the biological process of receiving cells [43]. Although there are abundant signaling modulation molecules (protein, RNA, lipid and DNA) contained in ADSC exosomes, the contents of miRNAs are relatively high in exosomes compared with other components due to the protective effect of exosomal miRNAs from degradation [13]. Therefore, ample miRNA contents in exosomes account for their multiple regulatory effects on recipient cells. A previous study indicated that miR-192-5p in ADSC exosomes could impair fibrosis in HSFs by targeting the IL-17RA/Smad axis [16]. In addition, miR-29b-3p in MSC

Downloaded from academic.oup.com/burnstrauma/article/doi/10.1093/burnst/tkad064/7676325 by guest on 13 October 2026

exosomes has been reported to suppress the proliferation of fibroblasts by downregulating FZD6 expression in idiopathic pulmonary fibrosis [44]. In this study, we found that several miR-125b-5p molecules are highly expressed in ADSC exosomes. By bioinformatics analysis and further replication experiments, we proved that miR-125b-5p in ADSC exosomes can regulate the expression of Smad2 and suppress fibrosis in myofibroblasts. miRNAs contained in different exosomes differ from one another. For instance, stem cell-derived exosomes are different from nonstem cell exosomes, exosomes from a morbid state are different from those from a healthy state, and exosomes from senescent cells are different from those from young cells. It is noteworthy that miR-125b-5p is highly expressed not only in ADSC exosomes but also in all kinds of MSCs, such as umbilical cord-derived mesenchymal stem cells (UC-MSCs) [45]. It has been reported that UC-MSC exosomal miRNAs, including miR-125b-5p, suppress myofibroblast differentiation by inhibiting the TGF-β/Smad2 pathway during wound healing [46]. miR-125b-5p is critical for fibroblast-to-myofibroblast transition and cardiac fibrosis [47]. Together with these studies, we found that ADSC exosomes could alleviate hypertrophic scars via suppression of Smad2 by specific delivery of miR-125b-5p.

Conclusions

In this study, we focused on the effect of ADSC exosomes on wound healing and hypertrophic scars. Our study demonstrated that ADSC exosomes could promote wound healing, improve healing quality and prevent scar formation. ADSC exosomes inhibited the expression of fibrosis-related molecules such as α-SMA, COL1 and COL3 and inhibited the transdifferentiation of myofibroblasts. We proved for the first time that highly expressed miR-125b-5p in ADSC exosomes directly downregulated the expression of Smad2 by binding to its 3′UTR in hypertrophic fibroblasts. *In vivo* experiments also revealed that ADSC exosomes could alleviate bleomycin-induced skin fibrosis and downregulate the expression of Smad2. We showed that miR-125b-5p in ADSC exosomes attenuated hypertrophic scar fibrosis by directly inhibiting Smad2, which provided a novel therapeutic strategy and elucidated the special mechanism for the clinical treatment of hypertrophic scars by ADSC exosomes.

Supplementary material

Supplementary material is available at *Burns & Trauma Journal* online.

Abbreviations

ADSC: Adipose-derived stem cells; BCA: Bicinchoninic acid; COL1: Collagen I; CCK8: Cell counting kit-8; DEGs: Differentially expressed genes; de–FBS: Remove fetal bovine serum; ECL: Enhanced chemiluminescence; FBS: Fetal bovine serum; H&E: Hematoxylin and eosin; DAPI: 4',6-diamidino-2-phenylindole; GAPDH: Glyceraldehyde-3-phosphate dehydrogenase; GO: Gene ontology; HS: Hypertrophic scarring; HSFs: Hypertrophic scar fibroblasts; MFI: Mean fluorescence intensity; MSC: Mesenchymal stem cell; 3′UTR: 3′Untranslated region; α-SMA: α-Smooth muscle actin; ECM: Extracellular matrix; IL-17: Interleukin-17; KEGG: Kyoto encyclopedia of genes and genomes; miR: MicroRNA; miR-125b-5p: MicroRNA-125b-5p; NTA: Nanoparticle tracking analysis; PBS: Phosphate-buffered saline; PVDF: Polyvinylidene difluoride; Smad2: Mothers against decapentaplegic homolog 2; TEM: Transmission electron microscopy; TBST: Tris buffered saline with tween 20; TGF: Transforming growth factor; UC-MSCs: Umbilical cord-derived mesenchymal stem cell; YAP/TAZ: Yes-associated protein/recombinant tafazzin protein.

Acknowledgments

The authors thank all the other members in their laboratory for their insights and technical support.

Funding

This work was supported by grants from the Medical Research Program of Xi'an City (2023YXYJ0185) and the Key Research and Development Program of Shaanxi Province (2022SF-047, 2022SF-044 and 2023-ZDLSF-24). The funding body played no role in the design of the study and in collection, analysis and interpretation of data and in the writing of the manuscript.

Authors' contributions

Conceptualization: DHH and KS; methodology (animal model: WZ, RW and CLX; formal analysis: YWW and RW; investigation: CLX, MYL and JZ; validation: HZ, YW and YGS; data curation: CY, LL and LXZ; writing—original draft preparation: CLX and HZ; writing—review and editing: KS and DHH; visualization: CH, YXC and YL; supervision: KS and CLX; project administration: DHH and XL; and funding acquisition: KS, CYT, KJW and DHH.

Ethics approval and consent to participate

All protocols involved with human samples in the study were approved by the Ethics Committee of Xijing Hospital, First Affiliated Hospital of Fourth Military Medical University (exosomes derived from human adipose mesenchymal stem cells attenuate hypertrophic scar fibrosis, KY20193244, March 2019). All animal experimental protocols were approved and performed in strict accordance with Experimental Animal Committee of Fourth Military Medical University (Xi'an, China).

Consent for publication

All authors approved the submission of the manuscript to this journal.

Conflict of interest

None declared.

Data availability

The data used to support the findings of this study are available from the corresponding author upon request.

References

1. Ung CY, Warwick A, Onoufriadis A, Barker JN, Parsons M, McGrath JA, *et al.* Comorbidities of keloid and hypertrophic

Downloaded from academic.oup.com/burnstrauma/article/doi/10.1093/burnst/tkad064/7676325 by guest on 13 October 2026

scars among participants in UK biobank. *JAMA Dermatol*. 2023;159:172–81.
2. Finnerty CC, Jeschke MG, Branski LK, Barret JP, Dziewulski P, Herndon DN. Hypertrophic scarring: the greatest unmet challenge after burn injury. *Lancet (London, England)*. 2016;388:1427–36.
3. Lee HJ, Jang YJ. Recent understandings of biology, prophylaxis and treatment strategies for hypertrophic scars and keloids. *Int J Mol Sci*. 2018;19:711. https://doi.org/10.3390/ijms19030711.
4. Ogawa R. The most current algorithms for the treatment and prevention of hypertrophic scars and keloids: a 2020 update of the algorithms published 10 years ago. *Plast Reconstr Surg*. 2022;149:79e–4.
5. Ogawa R. Keloid and hypertrophic scars are the result of chronic inflammation in the reticular dermis. *Int J Mol Sci*. 2017;18:606. https://doi.org/10.3390/ijms18030606.
6. Berman B, Maderal A, Raphael B. Keloids and hypertrophic scars: pathophysiology, classification, and treatment. *Dermatol Surg*. 2017;43:S3–s18.
7. Yin J, Zhang S, Yang C, Wang Y, Shi B, Zheng Q, *et al*. Mechanotransduction in skin wound healing and scar formation: potential therapeutic targets for controlling hypertrophic scarring. *Front Immunol*. 2022;13:1028410.
8. Shpichka A, Butnaru D, Bezrukov EA, Sukhanov RB, Atala A, Burdukovskii V, *et al*. Skin tissue regeneration for burn injury. *Stem Cell Res Ther*. 2019;10:94.
9. Zhang T, Wang XF, Wang ZC, Lou D, Fang QQ, Hu YY, *et al*. Current potential therapeutic strategies targeting the TGF-β/Smad signaling pathway to attenuate keloid and hypertrophic scar formation. *Biomed Pharmacother*. 2020;129:110287.
10. Wang J, Zhao M, Zhang H, Yang F, Luo L, Shen K, *et al*. KLF4 alleviates hypertrophic scar fibrosis by directly activating BMP4 transcription. *Int J Biol Sci*. 2022;18:3324–36.
11. Zhang J, Li Y, Bai X, Li Y, Shi J, Hu D. Recent advances in hypertrophic scar. *Histol Histopathol*. 2018;33:27–39.
12. Kalluri R, LeBleu VS. The biology, function, and biomedical applications of exosomes. *Science (New York, NY)*. 2020;367:eaau6977. https://doi.org/10.1126/science.aau6977.
13. Zhang J, Li S, Li L, Li M, Guo C, Yao J, *et al*. Exosome and exosomal microRNA: trafficking, sorting, and function. *Genomics Proteomics Bioinformatics*. 2015;13:17–24.
14. Wu P, Zhang B, Shi H, Qian H, Xu W. MSC-exosome: a novel cell-free therapy for cutaneous regeneration. *Cytotherapy*. 2018;20:291–301.
15. An Y, Lin S, Tan X, Zhu S, Nie F, Zhen Y, *et al*. Exosomes from adipose-derived stem cells and application to skin wound healing. *Cell Prolif*. 2021;54:e12993.
16. Li Y, Zhang J, Shi J, Liu K, Wang X, Jia Y, *et al*. Exosomes derived from human adipose mesenchymal stem cells attenuate hypertrophic scar fibrosis by miR-192-5p/IL-17RA/Smad axis. *Stem Cell Res Ther*. 2021;12:221.
17. Li C, Wei S, Xu Q, Sun Y, Ning X, Wang Z. Application of ADSCs and their exosomes in scar prevention. *Stem Cell Rev Rep*. 2022;18:952–67.
18. Wu ZY, Zhang HJ, Zhou ZH, Li ZP, Liao SM, Wu ZY, *et al*. The effect of inhibiting exosomes derived from adipose-derived stem cells via the TGF-β1/Smad pathway on the fibrosis of keloid fibroblasts. *Gland Surg*. 2021;10:1046–56.
19. Zhang W, Bai X, Zhao B, Li Y, Zhang Y, Li Z, *et al*. Cell-free therapy based on adipose tissue stem cell-derived exosomes promotes wound healing via the PI3K/Akt signaling pathway. *Exp Cell Res*. 2018;370:333–42.
20. Zhang J, Li Y, Liu J, Han F, Shi J, Wu G, *et al*. Adiponectin ameliorates hypertrophic scar by inhibiting yes-associated protein transcription through SIRT1-mediated deacetylation of C/EBPβ and histone H3. *iScience*. 2022;25:105236.
21. Shen K, Jia Y, Wang X, Zhang J, Liu K, Wang J, *et al*. Exosomes from adipose-derived stem cells alleviate the inflammation and oxidative stress via regulating Nrf2/HO-1 axis in macrophages. *Free Radic Biol Med*. 2021;165:54–66.
22. Shen K, Wang X, Wang Y, Jia Y, Zhang Y, Wang K, *et al*. miR-125b-5p in adipose derived stem cells exosome alleviates pulmonary microvascular endothelial cells ferroptosis via Keap1/Nrf2/GPX4 in sepsis lung injury. *Redox Biol*. 2023;62:102655.
23. Liu SY, Wu JJ, Chen ZH, Zou ML, Teng YY, Zhang KW, *et al*. The m(6)a RNA modification modulates gene expression and fibrosis-related pathways in hypertrophic scar. *Front Cell Dev Biol*. 2021;9:748703.
24. Son D, Harijan A. Overview of surgical scar prevention and management. *J Korean Med Sci*. 2014;29:751–7.
25. Moretti L, Stalfort J, Barker TH, Abebayehu D. The interplay of fibroblasts, the extracellular matrix, and inflammation in scar formation. *J Biol Chem*. 2022;298:101530.
26. Martin P, Nunan R. Cellular and molecular mechanisms of repair in acute and chronic wound healing. *Br J Dermatol*. 2015;173:370–8.
27. Monavarian M, Kader S, Moeinzadeh S, Jabbari E. Regenerative scar-free skin wound healing. *Tissue Eng Part B Rev*. 2019;25:294–311.
28. Bainbridge P. Wound healing and the role of fibroblasts. *J Wound Care*. 2013;22:10–2.
29. Driskell RR, Watt FM. Understanding fibroblast heterogeneity in the skin. *Trends Cell Biol*. 2015;25:92–9.
30. Thulabandu V, Chen D, Atit RP. Dermal fibroblast in cutaneous development and healing. *Wiley Interdiscip Rev Dev Biol*. 2018;7:10. https://doi.org/10.1002/wdev.307.
31. Karsdal MA, Nielsen SH, Leeming DJ, Langholm LL, Nielsen MJ, Manon-Jensen T, *et al*. The good and the bad collagens of fibrosis - their role in signaling and organ function. *Adv Drug Deliv Rev*. 2017;121:43–56.
32. Jiang D, Christ S, Correa-Gallegos D, Ramesh P, Kalgudde Gopal S, Wannemacher J, *et al*. Injury triggers fascia fibroblast collective cell migration to drive scar formation through N-cadherin. *Nat Commun*. 2020;11:5653.
33. Gibb AA, Lazaropoulos MP, Elrod JW. Myofibroblasts and fibrosis: mitochondrial and metabolic control of cellular differentiation. *Circ Res*. 2020;127:427–47.
34. Pakshir P, Noskovicova N, Lodyga M, Son DO, Schuster R, Goodwin A, *et al*. The myofibroblast at a glance. *J Cell Sci*. 2020;133:jcs227900. https://doi.org/10.1242/jcs.227900.
35. Brewer CM, Nelson BR, Wakenight P, Collins SJ, Okamura DM, Dong XR, *et al*. Adaptations in hippo-yap signaling and myofibroblast fate underlie scar-free ear appendage wound healing in spiny mice. *Dev Cell*. 2021;56:2722–40.e6.
36. Mia MM, Singh MK. New insights into hippo/YAP Signaling in fibrotic diseases. *Cell*. 2022;11:2065. https://doi.org/10.3390/cells11132065.
37. Zhang T, He X, Caldwell L, Goru SK, Ulloa Severino L, Tolosa MF, *et al*. NUAK1 promotes organ fibrosis via YAP and TGF-β/SMAD signaling. *Sci Transl Med*. 2022;14:eaaz4028.

Downloaded from academic.oup.com/burnstrauma/article/doi/10.1093/burnst/tkad064/7676325 by guest on 13 October 2026

38. Hu HH, Chen DQ, Wang YN, Feng YL, Cao G, Vaziri ND, *et al.* New insights into TGF-β/Smad signaling in tissue fibrosis. *Chem Biol Interact*. 2018;292:76–83.
39. Liu J, Jin J, Liang T, Feng XH. To Ub or not to Ub: a regulatory question in TGF-β signaling. *Trends Biochem Sci*. 2022; 47:1059–72.
40. Zi Z, Chapnick DA, Liu X. Dynamics of TGF-β/Smad signaling. *FEBS Lett*. 2012;586:1921–8.
41. Diener C, Keller A, Meese E. Emerging concepts of miRNA therapeutics: from cells to clinic. *Trends in genetics: TIG*. 2022; 38:613–26.
42. Ferragut Cardoso AP, Banerjee M, Nail AN, Lykoudi A, States JC. miRNA dysregulation is an emerging modulator of genomic instability. *Semin Cancer Biol*. 2021;76:120–31.
43. Fabian MR, Sonenberg N. The mechanics of miRNA-mediated gene silencing: a look under the hood of miRISC. *Nat Struct Mol Biol*. 2012;19:586–93.
44. Wan X, Chen S, Fang Y, Zuo W, Cui J, Xie S. Mesenchymal stem cell-derived extracellular vesicles suppress the fibroblast proliferation by downregulating FZD6 expression in fibroblasts via micrRNA-29b-3p in idiopathic pulmonary fibrosis. *J Cell Physiol*. 2020;235:8613–25.
45. Ma C, Qi X, Wei YF, Li Z, Zhang HL, Li H, *et al.* Amelioration of ligamentum flavum hypertrophy using umbilical cord mesenchymal stromal cell-derived extracellular vesicles. *Bioactive materials*. 2023;19:139–54.
46. Fang S, Xu C, Zhang Y, Xue C, Yang C, Bi H, *et al.* Umbilical cord-derived mesenchymal stem cell-derived Exosomal MicroRNAs suppress Myofibroblast differentiation by inhibiting the transforming growth factor-β/SMAD2 pathway during wound healing. *Stem Cells Transl Med*. 2016;5:1425–39.
47. Nagpal V, Rai R, Place AT, Murphy SB, Verma SK, Ghosh AK, *et al.* MiR-125b is critical for fibroblast-to-Myofibroblast transition and cardiac fibrosis. *Circulation*. 2016;133:291–301.

Downloaded from academic.oup.com/burnstrauma/article/doi/10.1093/burnst/tkad064/7676325 by guest on 13 October 2026